REPORT DOCUMENTATION PAGE

Form Approved
OMB No. 0704-0188

1. REPORT DATE *(DD-MM-YYYY)*	2. REPORT TYPE	3. DATES COVERED *(From - To)*
	Paper	

4. TITLE AND SUBTITLE	5a. CONTRACT NUMBER
	5b. GRANT NUMBER
	5c. PROGRAM ELEMENT NUMBER
6. AUTHOR(S)	5d. PROJECT NUMBER
	5e. TASK NUMBER
	5f. WORK UNIT NUMBER

7. PERFORMING ORGANIZATION NAME(S) AND ADDRESS(ES)	8. PERFORMING ORGANIZATION REPORT
Air Force Research Laboratory (AFMC) AFRL/PRSP 5 Pollux Drive Edwards AFB CA 93524-7048	
9. SPONSORING / MONITORING AGENCY NAME(S) AND ADDRESS(ES)	**10. SPONSOR/MONITOR'S ACRONYM(S)**
Air Force Research Laboratory (AFMC) AFRL/PRS 5 Pollux Drive Edwards AFB CA 93524-7048	**11. SPONSOR/MONITOR'S NUMBER(S)**

12. DISTRIBUTION / AVAILABILITY STATEMENT

Approved for public release; distribution unlimited.

13. SUPPLEMENTARY NOTES

14. ABSTRACT

15. SUBJECT TERMS

16. SECURITY CLASSIFICATION OF:			17. LIMITATION OF ABSTRACT	18. NUMBER OF PAGES	19a. NAME OF RESPONSIBLE PERSON
					Leilani Richardson
a. REPORT	b. ABSTRACT	c. THIS PAGE			19b. TELEPHONE NUMBER *(include area code)*
Unclassified	Unclassified	Unclassified	A		(661) 275-5015

Standard Form 298 (Rev. 8-98)
Prescribed by ANSI Std. 239.18

7 items enclosed

MEMORANDUM FOR PRS (In-House Publication)

FROM: PROI (STINFO) 12 July 2002

SUBJECT: Authorization for Release of Technical Information, Control Number: **AFRL-PR-ED-TP-2002-179**
Andrew Jamison (USC); Andrew Ketsdever (AFRL/PRSA), "Performance Comparisons of Underexpanded Orifices and DeLaval Nozzles at Low Reynolds Numbers"

AIAA Joint Propulsion Conference **(Statement A)**
(Indianapolis, IN, 08-11 July 2002) (Deadline: PAST due = 08 Jul 02)

1. This request has been reviewed by the Foreign Disclosure Office for: a.) appropriateness of distribution statement, b.) military/national critical technology, c.) export controls or distribution restrictions, d.) appropriateness for release to a foreign nation, and e.) technical sensitivity and/or economic sensitivity.
Comments:_____

Signature _____ Date _____

2. This request has been reviewed by the Public Affairs Office for: a.) appropriateness for public release and/or b) possible higher headquarters review.
Comments: _____

Signature _____ Date _____

3. This request has been reviewed by the STINFO for: a.) changes if approved as amended, b) appropriateness of references, if applicable; and c.) format and completion of meeting clearance form if required
Comments:_____

Signature _____ Date _____

4. This request has been reviewed by PR for: a.) technical accuracy, b.) appropriateness for audience, c.) appropriateness of distribution statement, d.) technical sensitivity and economic sensitivity, e.) military/ national critical technology, and f.) data rights and patentability
Comments:_____

APPROVED/APPROVED AS AMENDED/DISAPPROVED

_____

PHILIP A. KESSEL Date
Technical Advisor
Space and Missile Propulsion Division

Performance Comparisons of Underexpanded Orifices and DeLaval Nozzles at Low Reynolds Numbers

Andrew Jamison[‡]
University of Southern California
Department of Aerospace Engineering
Los Angeles, CA

Andrew D. Ketsdever[†]
Air Force Research Laboratory
Propulsion Directorate
Edwards AFB, CA

ABSTRACT

The popularity of micropropulsion system development has led to renewed interest in the determination of propulsive properties of orifice flows since micronozzle expansions may suffer high viscous losses at low pressure operation. The mass flow and relative thrust for an under expanded orifice is measured as a function of orifice stagnation pressure from 0.1 to 3.5 Torr. Nitrogen, argon, and helium propellant gases are passed through a 1.0 mm diameter orifice with a wall thickness of 0.015 mm . Near-free molecule, transitional and continuum flow regimes are studied. The relative thrust is determined by a novel thrust stand designed primarily for low operating pressure, micropropulsion systems. It is shown that the thrust indications obtained from the stand are a function of the facility background pressure, and corrections are made to determine the indicated thrust for a zero background pressure with nitrogen as propellant. Highly repeatable (within 1 %) indicated thrust measurements are obtained in the thrust range from 5 to 500 μN.

Nomenclature

a – speed of sound (m/sec)
A – area (m^2)
c(γ) – constant dependent on ratio of specific heats
c' – mean molecular thermal speed (m/sec)
C_D – discharge coefficient
d – diameter (m)
g – gravitational constant (= 9.8 m/sec^2)
Isp – specific impulse (sec)
k – Boltzmann's constant (= 1.38 x 10^{-23} J/K)
Kn – Knudsen Number
m – mass (kg)
$\dot{M}$ - mass flow (kg/sec)
n – number density (m^{-3})
p – pressure (Pa)

[†] Senior Research Engineer, Senior Member AIAA
[*] Research Assistant, Student Member AIAA
[‡] Department Chair, Fellow AIAA

Re – Reynolds Number
r_p – radius of penetration (m)
t – thickness (m)
T – temperature (K)

α - orifice transmission probability
γ - ratio of specific heats
λ - mean free path (m)
μ - viscosity (Ns/m^2)
ρ - mass density (kg/m^3)
Δ - thrust stand deflection (arb. units)

subscripts

b – facility background
fm – free molecule
L – limit (theoretical maximum)
meas – experimentally measured

o – stagnation region
p - plenum
t – orifice or nozzle throat property
theor - theoretical

superscripts

* - orifice plane (sonic) region

1. Introduction

In recent years, micropropulsion systems have been developed to address the need for highly mobile micro- and nanospacecraft. A wide array of concepts will require the expansion of propellant gases through microscale geometries (e.g. micronozzles). Because of the volume and power restrictions associated with storing or producing high pressures on micospacecraft, many micropropulsion systems will operate at relatively low pressures in the transitional flow regime.[1] The Reynolds number gives a measure of the flow efficiency in terms of viscous losses. The Reynolds number at a nozzle throat or an orifice is given by

$$\mathrm{Re}^* = \frac{\rho^* a^* d_t}{\mu^*} \qquad (1)$$

Lower Reynolds number implies higher viscous flow losses. Microspacecraft propulsion systems may inherently operate in low Reynolds number regions due to relatively low operating pressures and small characteristic dimensions.

Figure 1 shows the specific impulse as a function of distance through a conical micronozzle geometry with a throat diameter of $d_t = 27.7\ \mu m$. Navier-Stokes and Direct Simulation Monte Carlo numerical simulations have been performed at two different stagnation pressures $p_o = 10^6$ Pa and 10^5 Pa.[2] For cold gas operation (T_o = 300 K), the corresponding Reynolds numbers are 1300 and 130 respectively. As Fig. 1 shows, the specific impulse at the nozzle exit is approximately 14% higher than at the nozzle throat for Re^* = 1300. However, the specific impulse at the exit is only about 5% higher than at the nozzle throat for Re^* = 130. The reduction of efficiency in the micronozzle geometry as the Reynolds number decreases is due to viscous losses near the nozzle walls.

There is currently a large effort being devoted to the fabrication of micronozzles with throat diameters on the order of one to tens of micrometers (microns).[3-5] As Fig. 1 indicates, weighing the increase in performance versus fabrication complexity. At low Reynolds numbers, the micronozzle geometry may in fact degrade performance, and expansion of propellant from a simple thin walled orifice may be a good compromise between efficiency and system complexity. Some microelectro-mechanical systems (MEMS) fabricated nozzle geometries involve planar or rectangular throats (i.e. not axisymmetric).[3] Numerical studies have shown that flows generated near the side walls can result in even higher inefficiencies.[6]

The flow complexities from sonic orifices have been studied for several years.[7-11] However, the determination of the thrust generated from gas expanding through an orifice is an area that has received little attention. The advent of micropropulsion systems has renewed interest in the determination of propulsive properties of orifice flows since micronozzle expansions appear to have major viscous losses.

This manuscript explores the thrust generated by an orifice expansion at relatively low Reynolds number. Besides a propulsion system in its own right, these orifices are also being investigated as a reliable means of calibrating micro-Newton thrust stands.[12]

2. Theory

To assess the performance of the orifice expansion in terms of propulsive parameters, properties at the entrance plane of the orifice are calculated from known stagnation values. The ratios of pressure, density, temperature and velocity for inviscid flow are

$$\frac{p^*}{p_o} = \left[\frac{2}{\gamma+1}\right]^{\gamma/\gamma-1} \qquad (2)$$

$$\frac{\rho^*}{\rho_o} = \left[\frac{2}{\gamma+1}\right]^{1/\gamma-1} \qquad (3)$$

$$\rho_o = \frac{p_o m}{k T_o} \qquad (4)$$

$$\left(\frac{a^*}{a_o}\right)^2 = \frac{T^*}{T_o} = \frac{2}{\gamma+1} \quad (5)$$

The theoretical, inviscid flow value for the orifice mass flow is

$$\dot{M} = \rho^* a^* A_t \quad (6)$$

Viscous effects can be measured in terms of a discharge coefficient defined by

$$C_D = \frac{\dot{M}_{meas}}{\dot{M}_{theor}} \quad (7)$$

where $\dot{M}_{theor}$ is calculated from Eq. (6). The theoretical thrust produced by the orifice is then given by

$$\Im = \dot{M}_{theor} a^* + p^* A_t \quad (8)$$

$$\Im = \left(\frac{\rho^*}{\rho_o} + \frac{p^*}{p_o}\right) A_t = c(\gamma) p_o A_t \quad (9)$$

The constant $c(\gamma)$ is equal to 1.16 and 1.14 for γ = 1.4 and 1.67 respectively. Equation (8) is only valid for the relatively low stagnation pressure range under investigation in this study where the effects of the external flow expansion can be neglected. Therefore, it is expected that the thrust produced by the orifice gas flow is relatively independent of the propellant.

A measure of the propulsive efficiency is given by the specific impulse as

$$Isp^* = \frac{\Im}{\dot{M} g} = \frac{\sqrt{\frac{2(\gamma+1)}{\gamma}\frac{k}{m}T_o}}{g} \quad (10)$$

For free molecule flow, the Knudsen number defined by

$$Kn_t = \frac{\lambda_o}{d_t} \quad (11)$$

is relatively high (Kn $\geq$ 10). This is realized at very low stagnation pressure operation where the molecule mean free path is larger than the orifice diameter. The free molecule mass flow, thrust and specific impulse are given by

$$\dot{M}_{fm} = \alpha m \frac{n_o \bar{c}}{4} A_t = \alpha m n_o \frac{\sqrt{\frac{8kT_o}{\pi m}}}{4} A_t \quad (12)$$

$$\Im_{fm} = \alpha \frac{p_o}{2} A_t \quad (13)$$

$$Isp_{fm} = \sqrt{\frac{\pi}{2}\frac{k}{m}T_o} \quad (14)$$

For the thin walled orifice used in this study, the theoretical transmission probability through the orifice α is near unity.[11]

3. Experiment

The orifice used in this study has a diameter of d_t = 1.0 mm and a thickness of t_t = 0.015 mm giving a t/d = 0.015. For t/d = 0.015, the transmission probability (α in Eqs. (12) and (13)) is very close to unity.[13] The orifice is machined by conventional means in a Tantalum shim which is attached to an aluminum plenum as shown in Fig. 2. The aluminum plenums are attached to a torsional thrust stand shown in Fig 3. The thrust measurements involve sensing the angular displacement resulting from a torque (thrust force x radial distance) applied to a damped rotary system. The present method for detecting angular deflection is to measure the linear displacement at a known radial distance using a Macro Sensors, Inc. linear voltage differential transducer (LVDT). The total linear movement of the arm is approximately 0.5 mm for a 2mN thrust level which corresponds to less than 0.1° angular deflection. The detailed operational characteristics of this thrust stand is the topic of earlier work.[7]

The thrust stand is placed inside the CHAFF-II facility, a steel vacuum chamber pumped by a Roots blower system with a pumping speed of 2000 L/sec for nitrogen. Ultimate pressures achievable in CHAFF-II are approximately 1.0 x 10^{-4} Torr.

The propellant is introduced into the orifice plenum through an adjustable needle valve located downstream of an MKS® mass flow meter. In the experimental configuration, the mass flow meter operated in the continuum regime through the pressure range studied.

Nitrogen, argon and helium are used as propellant gases in this study.

4. Results

Figure 4 shows the discharge coefficient as a function of the Reynolds number for nitrogen and argon. At lower Reynolds number, the measured values should asymptotically approach the theoretical free molecule limit of 0.583 and 0.549 for $\gamma = 1.4$ and 1.67 respectively. For the range of Reynolds number shown in Fig. 4, the orifice stagnation pressure ranges from 0.1 to 3.5 Torr. The discharge coefficient asymptotes towards 0.9 for higher Reynolds number flows. The maximum discharge coefficient for nitrogen is consistent with previous studies which show that for sharp edged orifices ($t/d \sim 0.01$), the maximum discharge coefficient is approximately 0.9 for Re^* upwards of 10^4.[10]

Figure 5 shows typical thrust stand traces from the LVDT. The traces are for nitrogen at p_o = 0.1 and 3.5 Torr respectively. Using Eq. (8) with the measured mass flow and stagnation pressure, the theoretical range of thrust shown in Fig. 5 is from approximately 7.9 μN (p_o = 0.1 Torr) to 430 μN (p_o = 3.5 Torr). As indicated by the traces, the signal voltage at p_o = 0.1 Torr is approximately 15 to 20 times above the noise. In this study, the noise is generally dominated by the minimum resolution of the digitizer (i.e. bit noise) and not an intrinsic property of the thrust stand. This suggests that the thrust stand should be capable of measuring thrust levels below 1.0 μN with minor modifications.

The indicated thrust measurements obtained from the thrust stand have a standard deviation of 6.65×10^{-3} and 1.04×10^{-2} for five runs on nitrogen and argon at p_o = 1.0 Torr respectively. Based on the mean deflection of the stand, this translates to a statistical error of 0.59% for nitrogen and 0.95% for argon. In all, the standard deviation is within 1% of the mean deflections over the range of stagnation pressures from 0.1 to 3.5 Torr.

The measured linear deflection from the thrust stand mounted LVDT is shown as a function of orifice stagnation pressure for nitrogen propellant in Fig. 6. Similar plots are shown for argon and helium in Figs. 7 and 8 respectively. Figure 9 shows the nitrogen deflection as a function of mass flow.

Figure 10 shows the thrust stand deflection for both nitrogen and argon. Because the range of operating Reynolds number for argon and nitrogen are similar, the results overlap as expected from Eq. (9). However, the level of agreement only holds for propellants which have a similar Reynolds number for a given stagnation pressure (i.e. similar viscous effects as a function of p_o).

Because the orifice Reynolds number (Eq. (1)) is a factor of three lower for helium than nitrogen, it is expected that the helium thrust (deflection) level would be somewhat lower at a given stagnation pressure. The helium results are compared to nitrogen deflections in Fig. 11. As expected, the deflection is lower than that for nitrogen propellant at similar stagnation pressures due to higher viscous losses.

It is known that the deflection for a given orifice stagnation pressure is dependent on the background pressure of the facility. Figure 12 shows the measured deflection for given orifice stagnation pressures as a function of the chamber background pressure. The absolute deflection for a given stagnation pressure decreases as the background pressure increases. The slope and intercept of the data is used to correct the results in Fig. 6 to a zero background pressure in the following section.

5. Discussion

Indications of Rarefied Flow

Figure 13 shows the effects of different flow regimes on the measured thrust (deflection) from a sharp-edged orifice. At high Knudsen number, the measured thrust follows the free molecule theory solution (Eq. (13)). As the transitional flow regime is reached, the measured flux deviates from free molecule theory and begins to asymptote to the inviscid flow theory solution (Eq. (8)) as the continuum regime is reached. Because the discharge coefficient only reaches a maximum of approximately 0.9 for sharp-edged orifices (Fig. 4 and Ref. 10), the inviscid flow solution is never quite met.

For helium, the flow Knudsen number at p_o = 0.1 Torr is approximately 1.4. The helium deflection data in Fig. 14 shows the theoretical lines for free molecule and inviscid continuum thrust. The measured data is bounded by the free molecule and continuum solutions. At the lower

operating pressure, the data follows the free molecular slope and tends toward the inviscid continuum solution at higher pressures. The data does not reach the inviscid solution at the maximum Reynolds number (p_o = 3.5 Torr) of about 27.

Figure 15 shows a similar result for nitrogen propellant flows. The maximum Knudsen number reached is approximately 0.5 at p_o = 0.1 Torr. Therefore, only a slight indication of the data trending towards the rarefied solution is expected as shown in Fig. 15 for $p_o \leq 0.5$ Torr. At the higher operating pressures, the nitrogen indicated thrust closely follows the inviscid continuum solution. This is consistent with the discharge coefficient results shown in Fig. 4 which indicates a discharge coefficient near 0.85 for $Re^* > 40$.

Facility Background Pressure Corrections

Because the facility background pressure is made up of two components (laboratory air and propellant), corrections to the thrust stand deflections can only be approximated for the nitrogen flow cases where the propellant and the laboratory backgrounds are similar.

The mechanism for lower thrust deflection as a function of increased background pressure is shown schematically in Fig. 16. For no orifice flow, the background pressure exerts an equal force on the front and back sides of the orifice plenum (equilibrium). As flow is introduced through the orifice, the resulting jets acts like an ejector pump similar to that of the oil vapor in a vacuum diffusion pump.[13,14] Collisional "removal" of the background gas by the orifice plume results in a lower background pressure on the jet side of the plenum then on the back side. The pressure difference exerts a force on the orifice in a direction opposite of the thrust vector produced by the jet. Since the gas density in the plume is relatively high compared to the background gas density in the vicinity of the orifice, the source flow can effectively prevent background molecules from penetrating the orifice plume and striking the front surface of the orifice plenum for reasonable background pressures ($p_b < 1 \times 10^{-3}$ Torr).[15] This suggests that the deflection as a function of the background pressure should be linear as a first order approximation as Fig. 12 indicates, or

$$\frac{d\Delta}{dp_b} = \text{constant}$$

$$\left(\Delta_{p_b=0}\right) - \left(\Delta_{p_b}\right) = p_b A_{eff} \qquad (15)$$

The effective area, A_{eff}, is a measure of the area being utilized to cause the deflection opposite to the thrust vector. Assuming that the background pressure in front of the orifice plenum is zero, the force exerted on the back side of the orifice plenum (A_p = 22.75 cm^2) is approximately 100 μN for $p_b = 3.3 \times 10^{-4}$ Torr. Therefore, the background pressure "negative thrust" effect can be a significant fraction of total "positive thrust" produced by the orifice.

Figure 17 shows the nitrogen thrust stand deflection for a corrected zero background pressure. This data is derived from the slopes of the deflection versus background pressure curves in Fig. 12 and the data obtained in Fig. 6.

6. Conclusions

The maximum of the discharge coefficient in this study was approximately 0.86 indicating that viscous effects are present throughout the operational pressure range. The momentum flux measurements from a sharp-edged orifice (t/d = 0.015) show a linear dependence on the stagnation pressure and mass flow for $Re^* > 20$. In this Reynolds number range, the data approaches the inviscid flow solution. Below $Re^* = 20$, rarefied effects begin to influence the thrust results, and the data approaches the free molecule theoretical solution as seen in the deflection data for helium at low stagnation pressure.

The thrust stand deflection is a function of the facility background pressure. Corrections to the deflection data must be made by extrapolating to a zero background pressure condition. The correction is upwards of about 40%. Operating the thrust stand with at least an order of magnitude lower ultimate facility pressure is desired.

Highly repeatable (within 1 %) indicated thrust measurements are obtained in the thrust range from 5 to 500 μN. There is also data to suggest that the thrust stand will be capable of measuring thrust levels below 1.0 μN with minor modifications.

An orifice which achieves discharge coefficients near unity can be used as a calibration source for thrust stand measurements. An orifice has the advantage of being able to obtain in-situ calibration without moving parts. The accuracy of the results may be much higher than traditional means of thrust stand calibration since the inviscid flow solutions are expected to be accurate for $C_D \sim 1$ and the flow can be simulated numerically as well.

7. Acknowledgements

The authors wish to thank Mr. Brian Bjelde for his assistance with the thrust stand and data reduction.

8. References

1. Ketsdever, A., "System Considerations and Design Options for Microspacecraft Propulsion Systems," in Micropropulsion for Small Spacecraft, AIAA Progress Series in Astronautics and Aeronautics, eds. Micci and Ketsdever, Vol. 187, 2000, pp. 139-166.

2. Ivanov, M., Markelov, G., Ketsdever, A., Wadsworth, D., "Numerical Study of Cold Gas Micronozzle Flows," AIAA paper 99-0166, January, 1999.

3. Bayt, R., Breuer, K., "Fabrication and Testing of Micron-Sized Cold-Gas Thrusters," in Micropropulsion for Small Spacecraft, AIAA Progress Series in Astronautics and Aeronautics, eds. Micci and Ketsdever, Vol. 187, 2000, pp. 381-398.

4. Janson, S., Helvajian, H., "Batch-Fabricated Microthrusters: Initial Results," AIAA paper 96-2988, July 1996.

5. Kohler, J., Jonsson, M., Simu, U., Stenmark, L., "Mass Flows of Fluidic Components for Cold Gas Thruster Systems," Micro/Nanotechnology for Space Applications, Pasadena, CA, April 1999.

6. Alexeenko, A., Gimelshein, S., Levin, D., Collins, R., "Numerical Modeling of Axisymmetric and Three-Dimensional Flows in MEMS Nozzles," AIAA paper 00-3668, July 2000.

7. Ashkenas, H., Sherman, F., "The Structure and Utilization of Supersonic Free Jets in Low Density Wind Tunnels," in Rarefied Gas Dynamics, Proceedings of the 4th International Symposium, ed. de Leeuw, Vol. 2, 1966, pp. 84-105.

8. Sreekanth, A., Prasad, A., Prasad, D., "Numerical and Experimental Investigations of Rarefied Gas Flows Through Nozzles and Composite Systems," in Rarefied Gas Dynamics, Proceedings of the 17th International Symposium, ed. Beylich, 1991, pp. 987-994.

9. Rebrov, A., "Free Jets in Vacuum Technologies," J. Vac. Sci. and Technol. A, to be published.

10. Smetana, F., Sherrill, W., Schort, D., "Measurements of the Discharge Characteristics of Sharp-Edged and Round-Edged Orifices in the Transition Regime," in Rarefied Gas Dynamics, Proceedings of the 5th International Symposium, ed. Brundin, Vol. 2, 1967, pp. 1243-1256.

11. Livesey, R., "Flow of Gases Through Tubes and Orifices," in Foundations of Vacuum Science and Technology, ed. Lafferty, 1998, pp. 81-140.

12. Tew, J., VanDenDriessche, J., Lutfy, F., Muntz, E.P., Wong, J., Ketsdever, A., "A Thrust Stand Designed for Performance Measurements of the Free Molecule Micro-Resistojet," AIAA paper 2000-3673, July 2000.

13. Dayton, B., "Diffusion and Diffusion-Ejector Pumps," in Foundations of Vacuum Science and Technology, ed. Lafferty, 1998, pp. 175-232.

14. Rebrov, A., "Studies on Physical Gas Dynamics of Jets as Applied to Vacuum Pumps," in Rarefied Gas Dynamics, Proceedings of the 15th International Symposium, ed. Teubner, 1986, pp. 455-473.

15. Muntz, E.P., Hamel, B.B., Maguire, B.L., "Some Characteristics of Exhaust Plume Rarefaction," AIAA J., Vol. 8, No. 9, 1970, pp. 1651-1658.

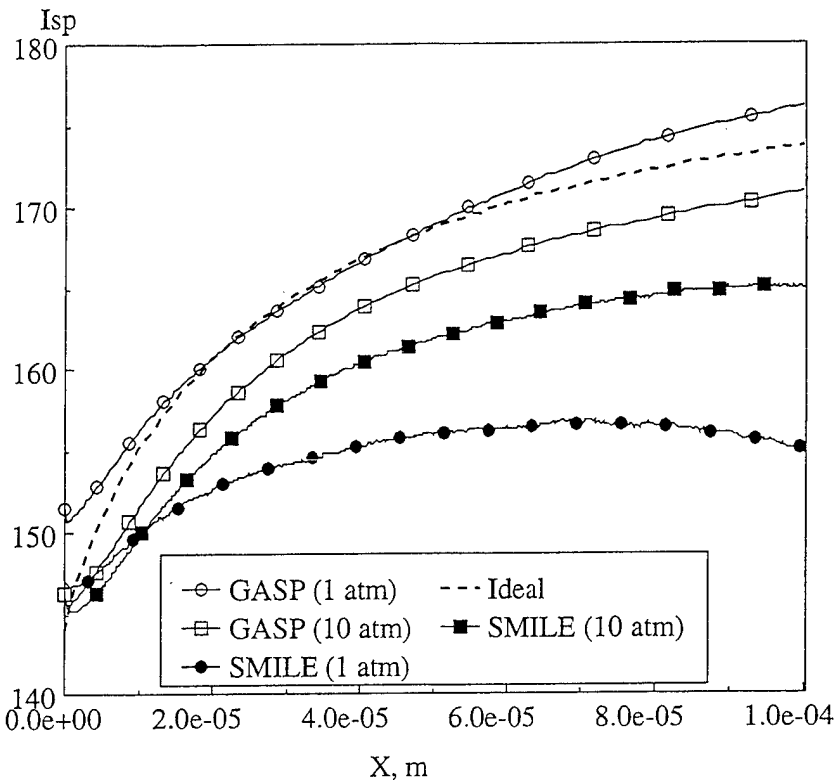

Fig. 1: Specific impulse along the axis of a MEMS fabricated micronozzle. (ref. 1)

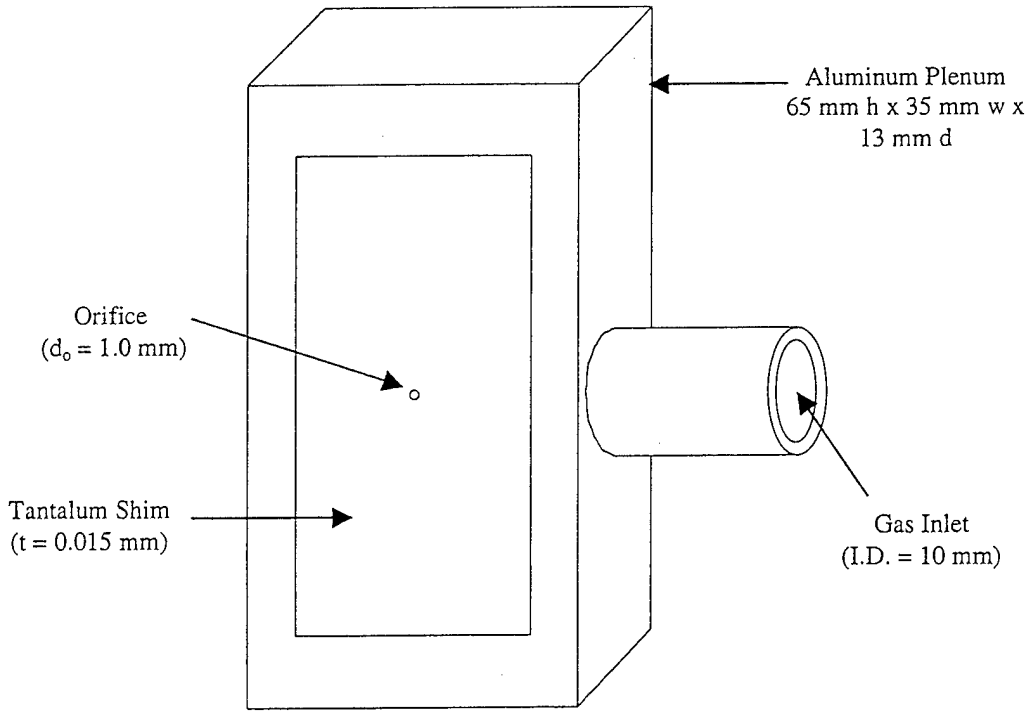

Fig. 2: Orifice geometry (t/d = 0.015).

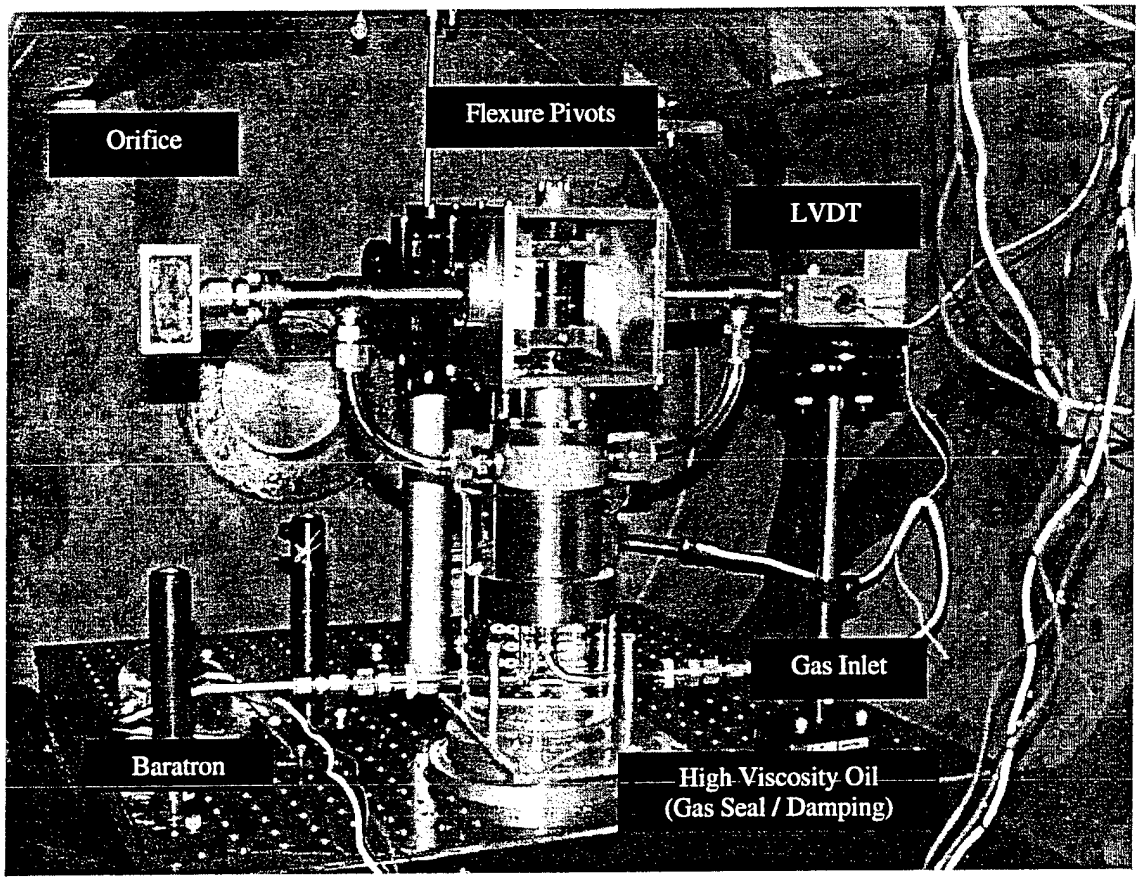

Fig. 3: Micro-Newton thrust stand installed in CHAFF-II vacuum facility.

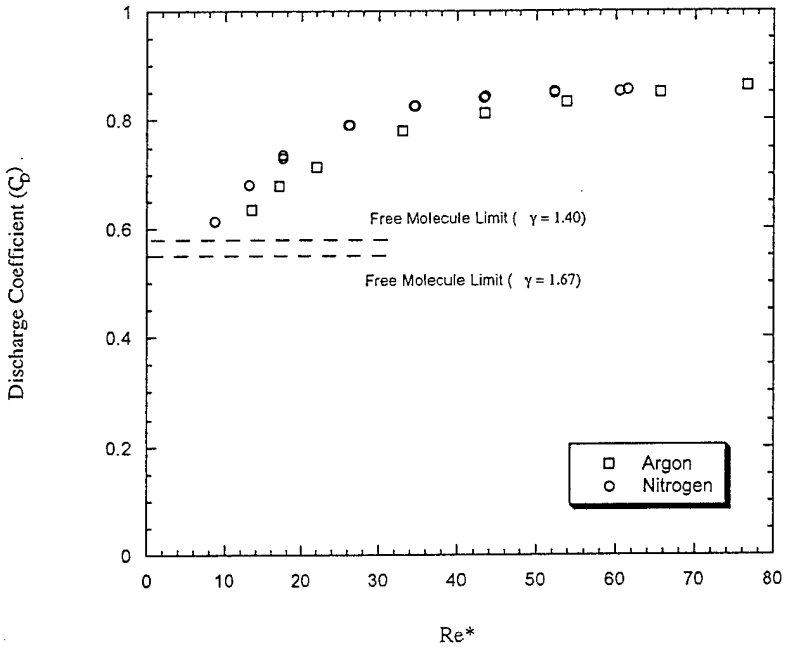

Fig. 4: Discharge coefficient as a function of orifice Reynolds number for argon and nitrogen gas flows.

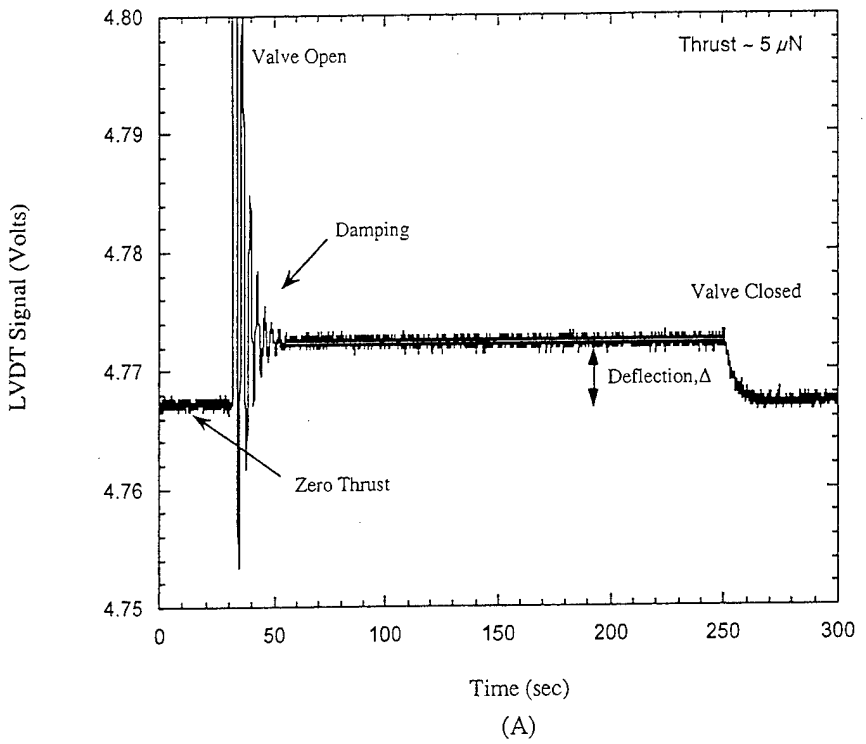

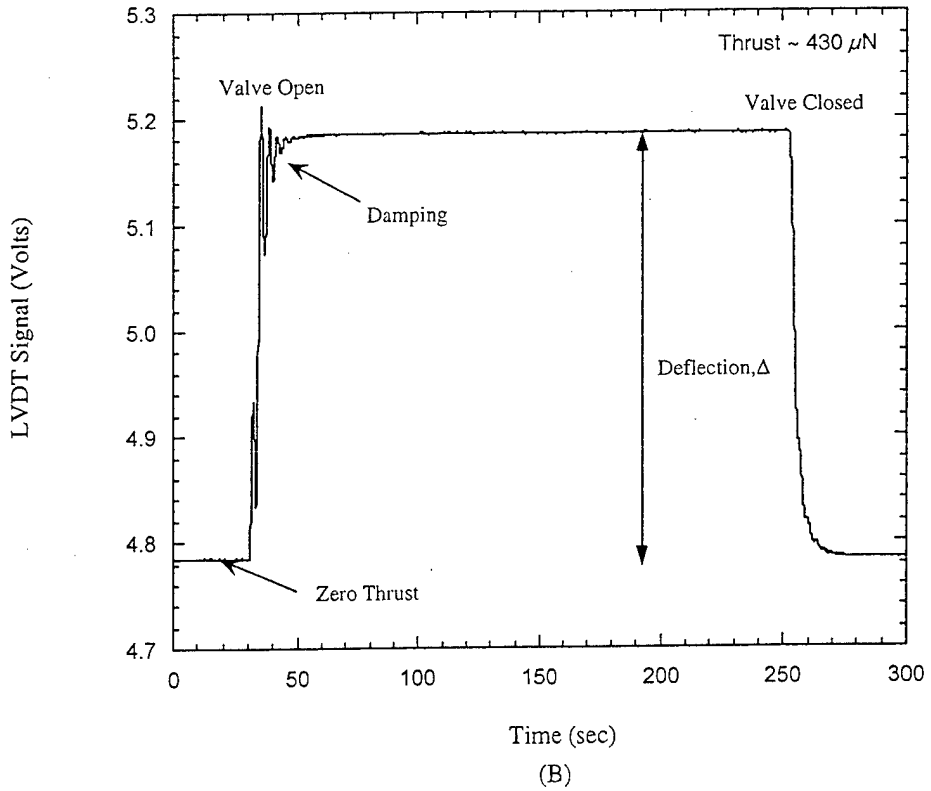

Fig. 5: LVDT signal from thrust stand. (A) Nitrogen flow, p_o = 0.1 Torr; (B) Nitrogen flow, p_o = 3.5 Torr.

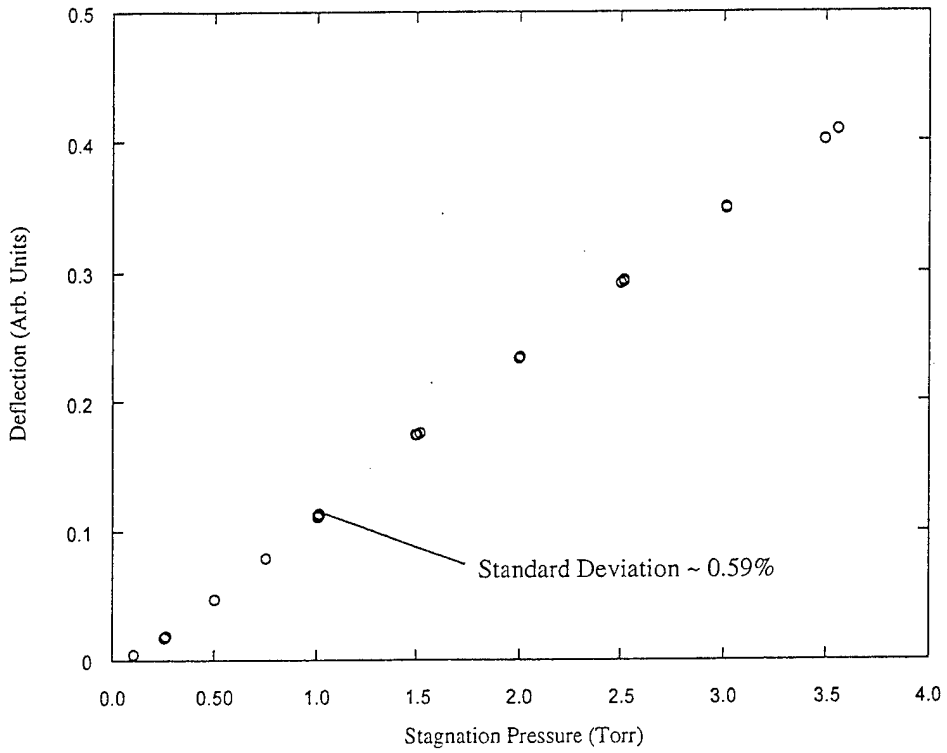

Fig. 6: Deflection as a function of stagnation pressure for nitrogen.

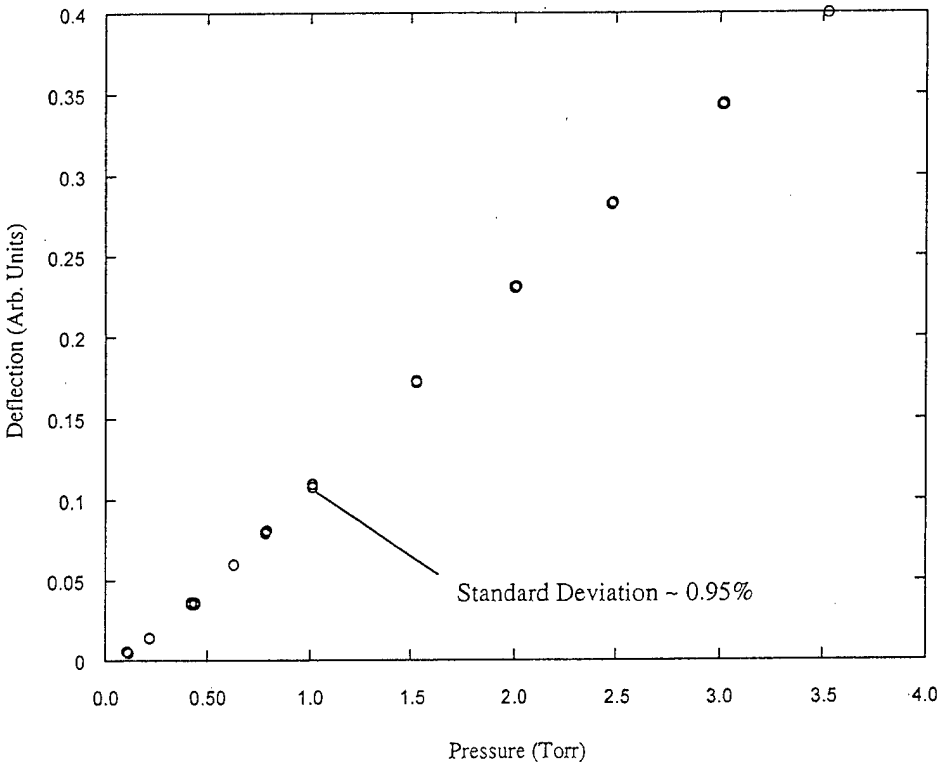

Fig. 7: Deflection as a function of stagnation pressure for argon.

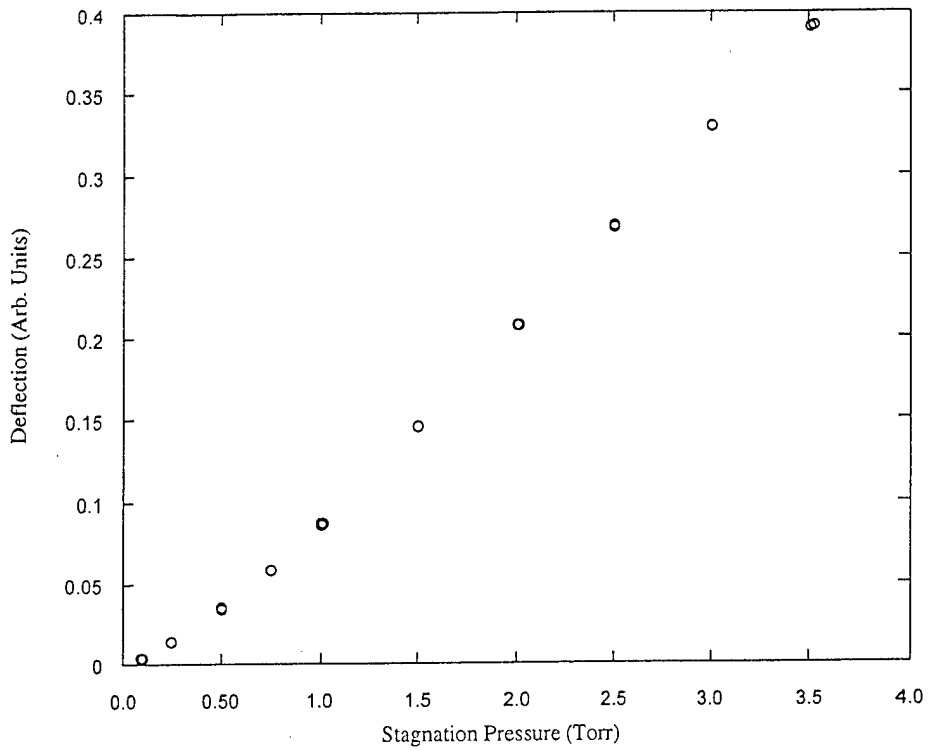

Fig. 8: Deflection as a function of stagnation pressure for helium.

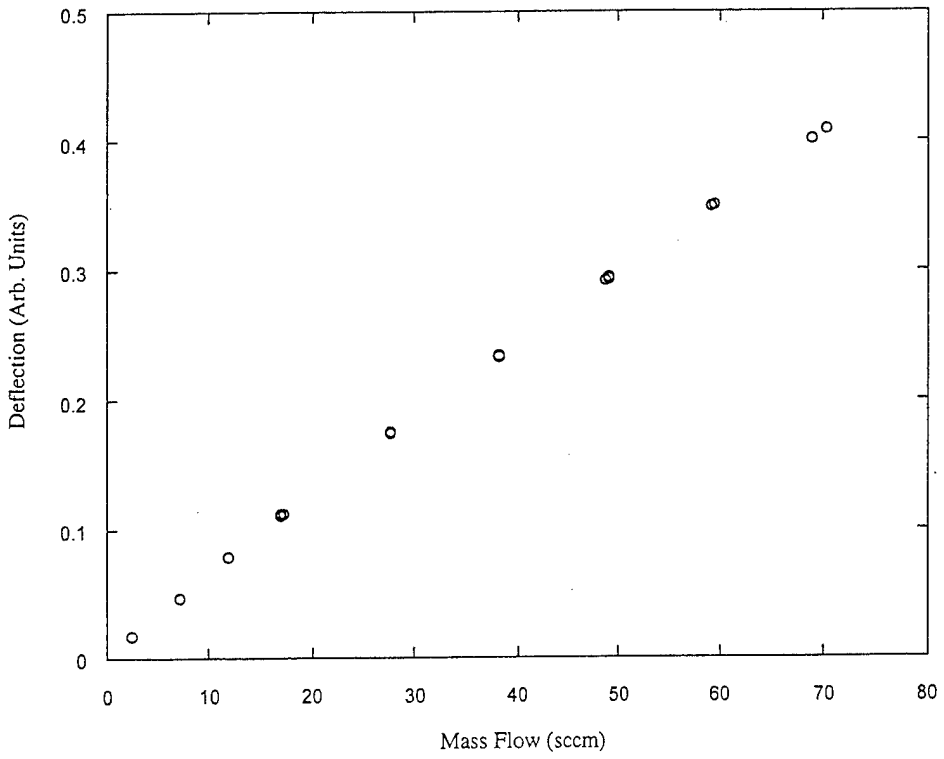

Fig. 9: Deflection as a function of mass flow for nitrogen.

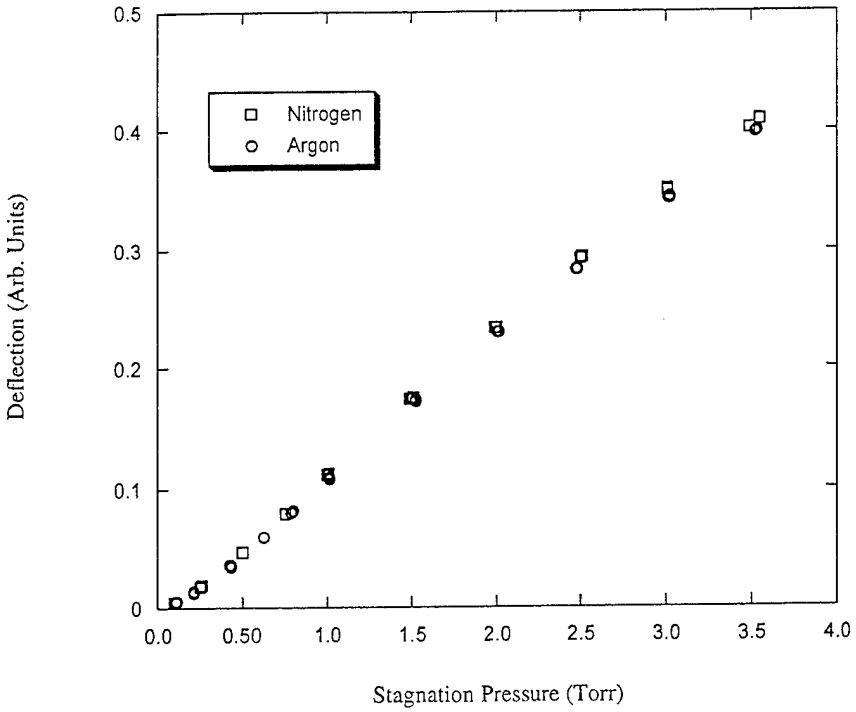

Fig. 10: Deflection as a function of stagnation pressure for nitrogen and argon gas flows.

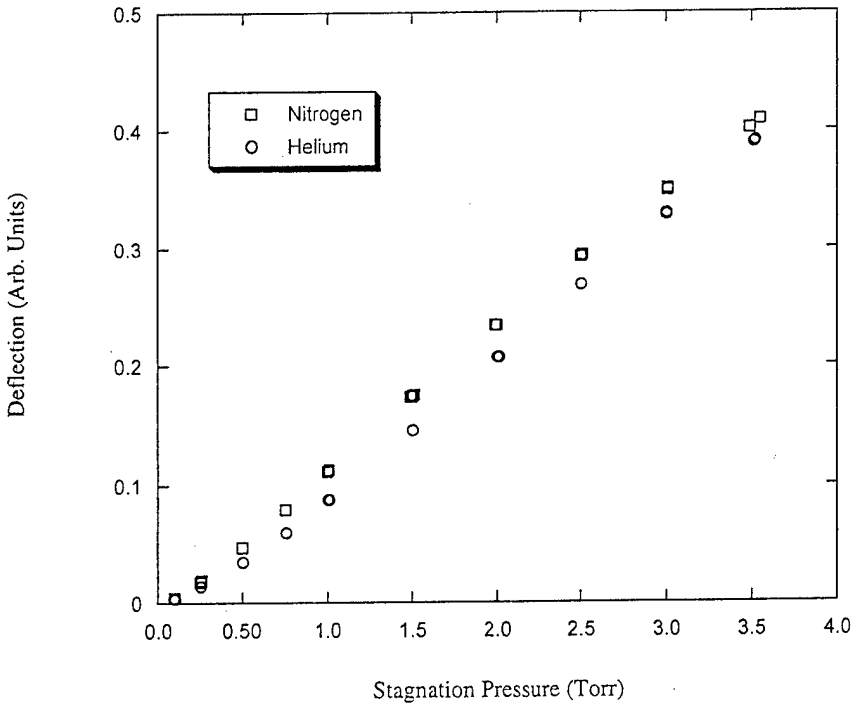

Fig. 11: Deflection as a function of stagnation pressure for nitrogen and helium.

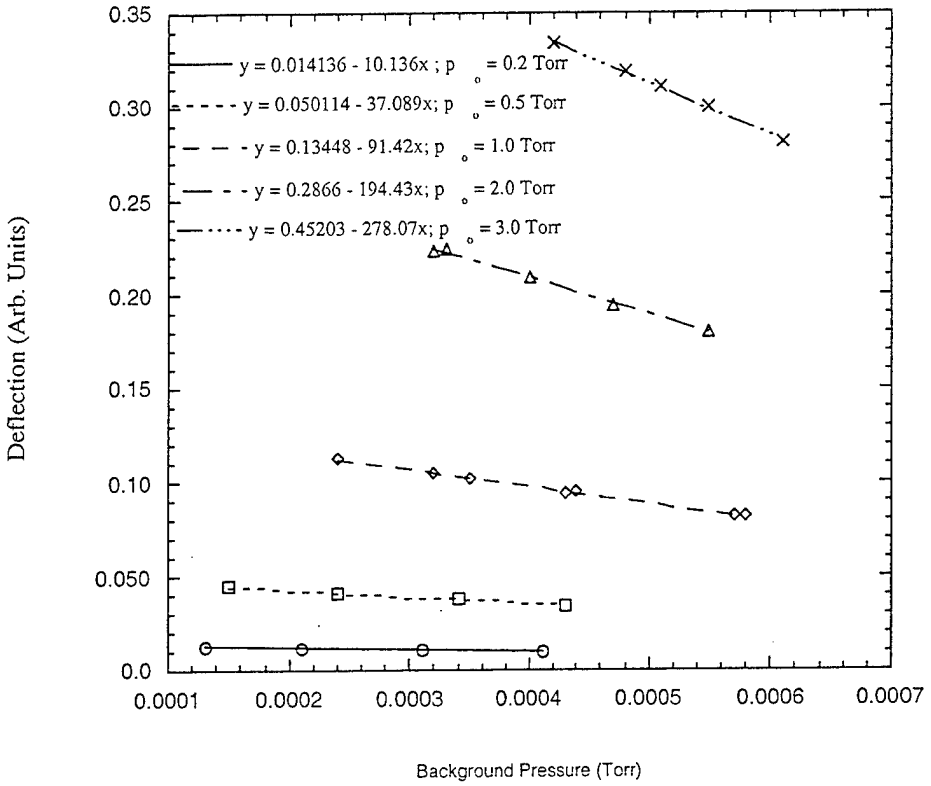

Fig. 12: Deflection as a function of chamber background pressure for nitrogen gas flows.

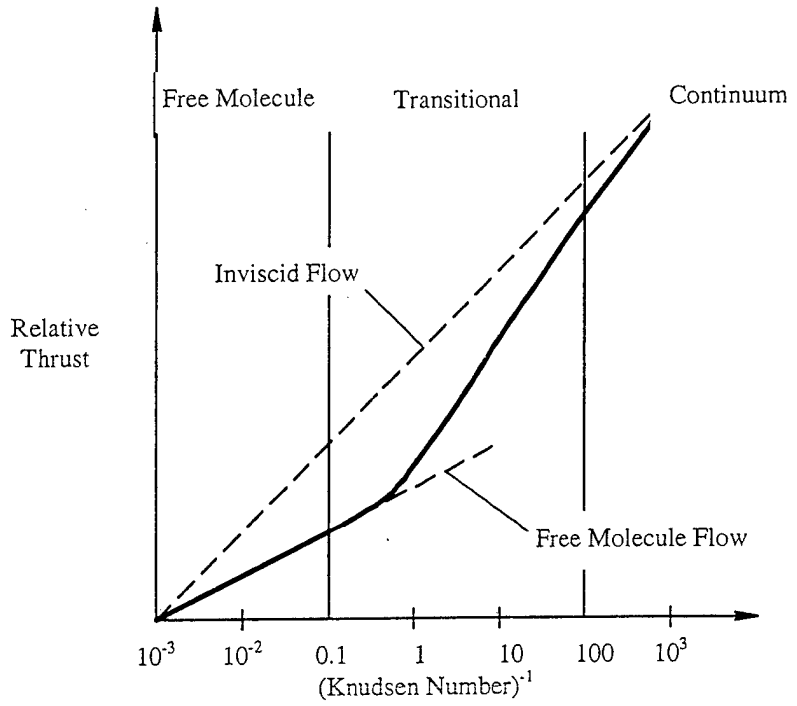

Fig. 13: Illustration of flow regime effects on the measured relative thrust.

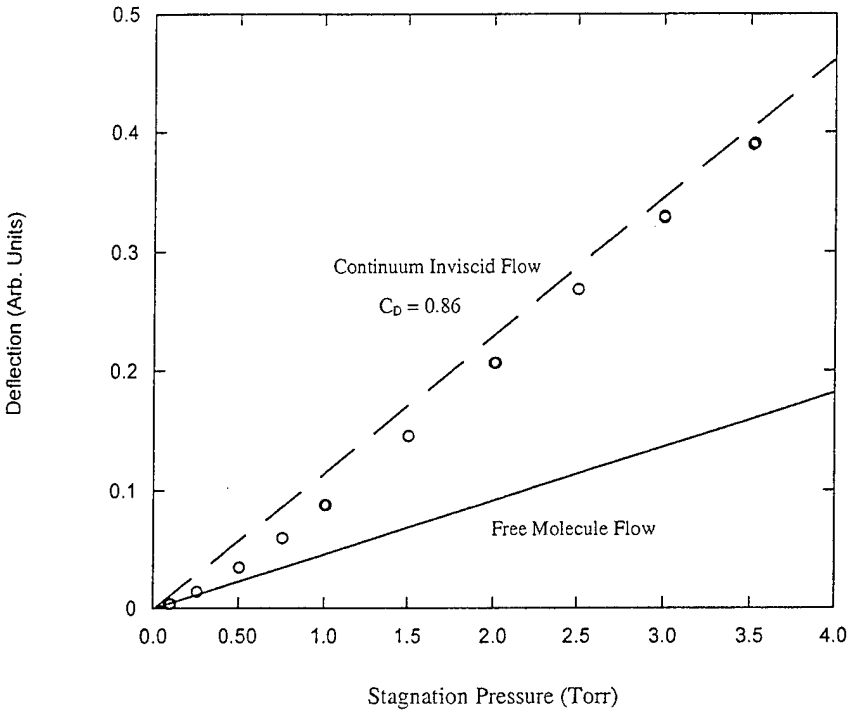

Fig. 14: Deflection as a function of stagnation pressure for helium.

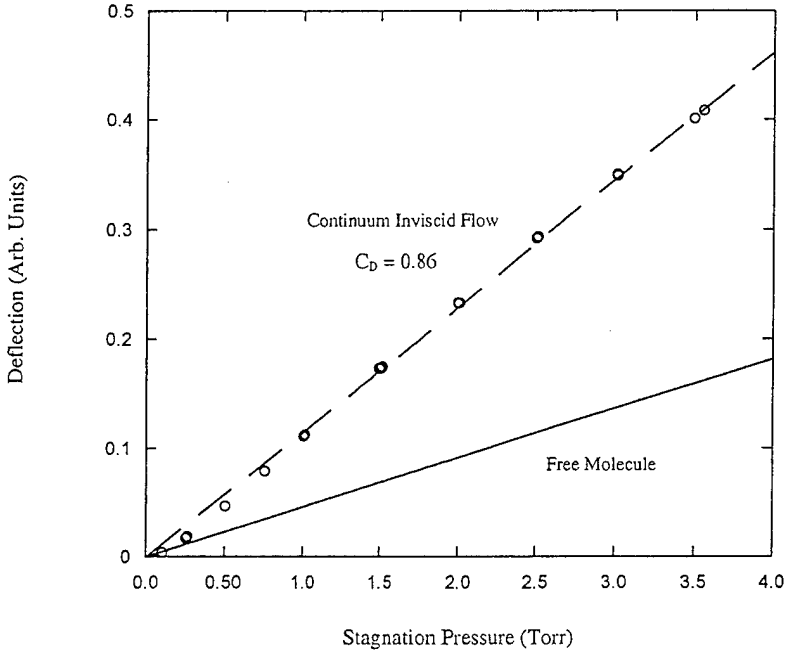

Fig. 15: Deflection as a function of stagnation pressure for nitrogen gas flow.

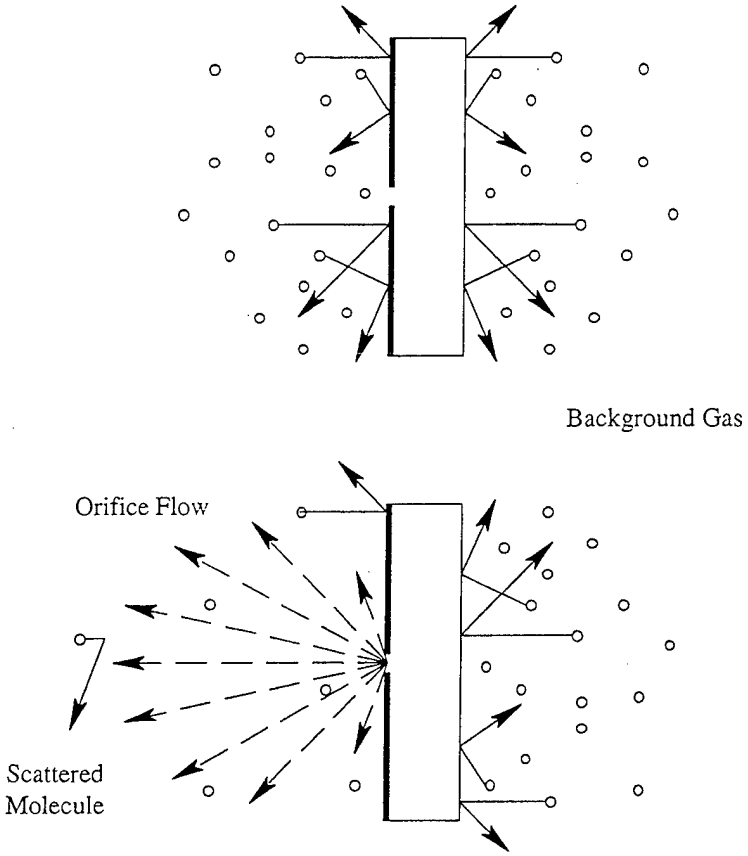

Fig. 16: Background pressure thrust degradation mechanism.

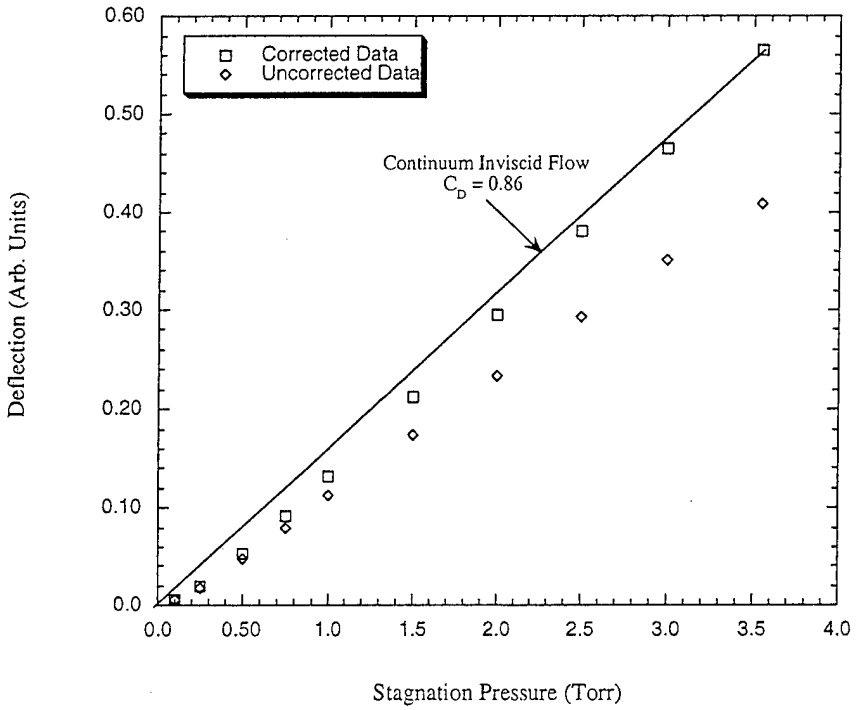

Fig. 17: Corrected deflection to zero background pressure for nitrogen.